Available online at www.sciencedirect.com
SCIENCE DIRECT®
Journal of Magnetic Resonance 163 (2003) 182–187
JMR Journal of Magnetic Resonance
www.elsevier.com/locate/jmr

REDOR with a relative full-echo reference

Anil K. Mehta, Lynette Cegelski, Robert D. O'Connor, and Jacob Schaefer*

Department of Chemistry, Washington University, One Brookings Dr., Campus Box 1134, St. Louis, MO 63130, USA

Received 14 November 2002; revised 24 February 2003

Abstract

REDOR and REDOR-like $^{13}C\{^{19}F\}$ and $^{2}H\{^{19}F\}$ NMR experiments have been performed on lyophilized whole cells of *Staphylococcus aureus*. The bacteria were grown to maturity on media containing L-[$^{13}C_3$]alanine or L-[methyl-d_3]alanine, and then complexed with the 4-fluorobiphenyl derivative of chloroeremomycin, an analogue of the widely used antibiotic, vancomycin. The position of the ^{19}F of the drug bound in the bacterial cell wall was determined relative to L-alanine ^{13}C and ^{2}H labels in the peptidoglycan peptide stem that was closest to the fluorinated biphenyl moiety of the drug. These determinations were made by dipolar recoupling methods that do not require an absolute measurement of the REDOR full echo (the signal observed without rotor-synchronized dephasing pulses) of the labels in the peptide stem.

1. Introduction

Understanding the antibiotic mode of action of various fluoro-substituted analogues of vancomycin starts with characterization of the binding of the drug to its target or targets in the bacterial cell wall. However, if the cell wall is thin or otherwise compromised, separation of the cell wall from the whole cell for analysis is not practical. Qualitatively, the proximity of the ^{19}F of the drug and a cell-wall ^{13}C, ^{15}N, or ^{2}H label is readily determined in whole cells using rotational-echo double-resonance [1]. However, a complication for the quantitative use of REDOR is that the exogenous ^{13}C, ^{15}N, and ^{2}H-labeled amino acids are incorporated into *both* cell walls and cytoplasmic proteins. The echo signals from labels in cytoplasmic proteins make the general determination of S_0 (the signal observed without rotor-synchronized dephasing pulses) for the cell wall impossible. Without the appropriate S_0, accurate distances of isolated spin-pairs cannot be extracted from REDOR dephasing. In this situation, however, it is still possible to determine the orientation of the dephasing spin relative to a cluster of ^{13}C spins, or the orientation of the vector connecting the dephasing and observed spins relative to the chemical-shift or quadrupolar tensor of the observed spin. In this paper, we show that these determinations can be made without the necessity of accurately determining an absolute S_0. The resulting generally applicable strategy makes feasible solid-state NMR structural measurements in many complicated, heterogeneous biological systems, including bacterial whole cells.

The stable-isotope labeling of growing and dividing cells of *Staphylococcus aureus* is efficient because of the ready incorporation of alanine, glycine, and lysine from the growth medium [2]. This means that ^{13}C, ^{15}N, and ^{2}H labels in these amino acids are incorporated into the stems, bridges, bridge-links, and cross-links of the cell-wall peptidoglycan [2], as well as in all cytoplasmic proteins. Potent antibiotics of *S. aureus* include the fluoro-substituted analogues of vancomycin produced by Eli Lilly [3]. In a mature cell, these drugs bind to D-alanine–D-alanine carboxyl termini of stems throughout the multi-layered peptidoglycan [4]. In a dividing cell, the drugs appear to form complexes preferentially with the D-alanine–D-alanine carboxyl termini of the peptidoglycan precursors: possibly with *N*-acetylglucosamine-*N*-acetyl-muramyl-pentapeptide-pyrophosphoryl-undecaprenol (lipid II), located in the cell wall just outside the cell membrane [5]. Binding of a vancomycin analogue to lipid II could interfere with transglycosylase activity and possibly transpeptidase activity as well [6]. The former extends the glycan main chain and the latter cross-links the

* Corresponding author. Fax: 1-314-935-4481.
E-mail address: schaefer@wuchem.wustl.edu (J. Schaefer).

1090-7807/03/$ - see front matter © 2003 Elsevier Science (USA). All rights reserved.
doi:10.1016/S1090-7807(03)00078-8

peptide stems. Both are essential for the synthesis of new cell wall.

2. Experimental details

Solid-state NMR was performed using a six-frequency transmission-line probe [7] having a 12-mm long, 6-mm inside-diameter analytical coil and a Chemagnetics/Varian ceramic stator. Lyophilized samples were contained in thin-wall Chemagnetics/Varian 5-mm outside-diameter zirconia rotors. The spectrometer was controlled by a Tecmag pulse programmer. Radiofrequency pulses for ^{13}C (125 MHz) and ^{2}H (76.8 MHz) were produced by 2-kW American Microwave Technology power amplifiers; ^{1}H (500 MHz) and ^{19}F (470 MHz) radiofrequency pulses were generated by 1-kW Amplifier Systems tube amplifiers driven by 50-W American Microwave Technology power amplifiers. The π-pulse lengths were 8 μs for ^{13}C and ^{2}H, and 5 μs for ^{19}F. Standard XY-8 phase cycling [8] was used for all dephasing pulses. A 12-T static magnetic field was provided by an 89-mm bore Magnex superconducting solenoid. Proton-carbon cross-polarization transfers were made in 2 ms at 62.5 kHz. Proton dipolar decoupling was 100 kHz during data acquisition; TPPM of the ^{1}H radiofrequency [9] was used throughout both dipolar evolution and acquisition periods.

REDOR and the REDOR-like experiment called RDX (for REDOR of clusters having a total of x spins) were each done in two parts [1,10], once with rotor-synchronized ^{19}F dephasing pulses (S) and once without (S_0). The dephasing pulses change the sign of the heteronuclear dipolar coupling, and this interferes with the spatial averaging resulting from the motion of the rotor. The difference in signal intensity ($\Delta S = S_0 - S$) for the observed spin is directly related to the corresponding distance to the dephasing spin. REDOR has found applications in the characterization of binding sites of proteins [11–13], and in the analysis of heterogeneous biological materials such as amyloid plaques [14], membrane protein helical bundles [15,16], insect cuticle [17], bacterial cell walls [18], and spider silk [19]. The analysis of RDX dephasing is more complicated because of coherences generated by the mix of π and $\pi/2$ pulses and incomplete removal of the ^{13}C–^{13}C isotropic J couplings. Distances are extracted from RDX dephasing by comparing the experimental results to multi-spin simulations [10] using SIMPSON [20].

Growth and harvest conditions for labeled *S. aureus* have been described [21]. Whole cells of *S. aureus* were grown, labeled by L-[$^{13}C_3$]alanine or L-[methyl-d_3]alanine in the presence of 5 μg/mL alaphosphin (a racemase inhibitor to stop scrambling of label between D- and L-alanines). Washed cells from a 400 mL growth, harvested at OD_{660} 1.0, were resuspended in 12 mL of

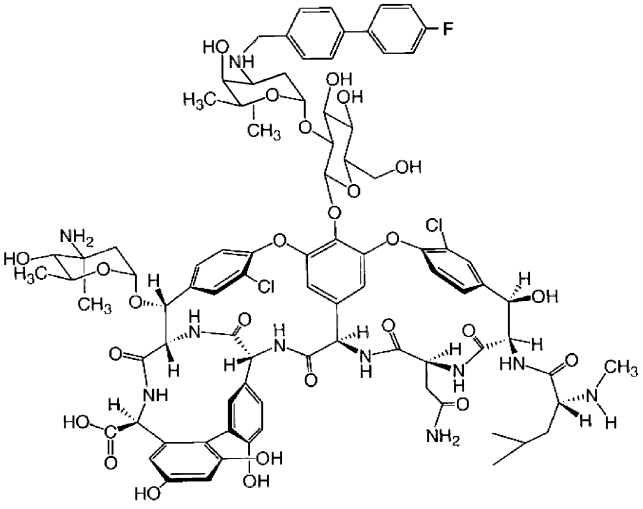

Fig. 1. The chemical structure of the 4-fluorobiphenyl derivative of chloroeremomycin (Eli Lilly and Co., compound no. LY329332), a vancomycin analogue.

40 mM triethanolamine and complexed with 2.7 μmol of Eli Lilly compound LY329332 (Fig. 1). This is sufficient to bind approximately one-third of the available cell-wall sites and constitutes a therapeutic dosage level [21]. The complexed sample was frozen and lyophilized.

3. Carbon-cluster labeling and RDX

One strategy to obtain orientational information from whole-cell complexes without knowing exact distances is to use ^{13}C cluster labeling of amino acids with detection by the modified REDOR sequence, RDX [10]. An outline of the RDX pulse sequence (Fig. 2) combines π pulses (to refocus chemical shifts in Hahn echoes) with $\pi/2$ pulses (to refocus J couplings in solid echoes). Unlike methods that utilize tailored, frequency-selective π pulses [22], the RDX sequence results in difference and

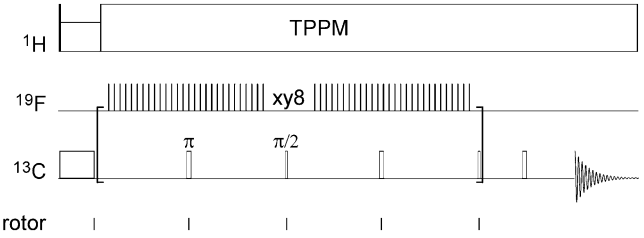

Fig. 2. Pulse sequence for REDOR of clusters (RDX) using eight refocusing ^{13}C pulses. The spacing between ^{13}C pulses is nT_r, where $n = 1, 2, 3, \ldots$ The four pulses within the square bracket are repeated twice. The last ^{13}C π pulse in the sequence is part of a two-rotor-cycle Hahn echo. All dephasing pulses are on the ^{19}F channel at the half and full rotor period. No ^{19}F pulse overlaps a ^{13}C pulse. Phases of the ^{13}C pulses follow the RDX scheme ([10]). Phases of the ^{19}F pulses follow the standard xy8 alternation scheme. Two-pulse phase modulation of the ^{1}H RF is used throughout evolution and decoupling periods.

full-echo spectra that are all in phase. RDX also provides distances (or in the case of whole cells, relative distances, and therefore orientation) between multiple spins in a single experiment. From the simultaneous measurement of relative dephasing rates, the orientation of the ^{13}C cluster can be determined. A disadvantage of RDX is that the total refocusing and dephasing relative to that obtained by REDOR for an isolated spin-pair, or frequency-selective REDOR for a selected pair within a cluster, are reduced [10]. The method of choice for a cluster of ^{13}C labels therefore varies with the size of the cluster. Frequency-selective REDOR has better sensitivity for pairs of ^{13}C labels, while RDX has better sensitivity for clusters of four or more ^{13}C labels.

Whole cells of *S. aureus*, labeled by L-[$^{13}C_3$]alanine and then complexed to Eli Lilly compound LY329332, show RDX difference peaks from all three labeled carbons (Fig. 3). In the cell wall, L-alanine is located at the base of each peptidoglycan peptide stem. However, only one stem is proximate to the ^{19}F of LY329332 [21]. Thus, the RDX difference peaks of Fig. 3 arise from just this nearest-neighbor L-alanine in the bacterial cell wall. The S_0 signal, on the other hand, arises from all the L-alanines in the cell wall, as well as from all the L-alanines incorporated in both cell wall and cytoplasmic proteins.

Comparison of four-spin calculations for the [$^{13}C_3$]alanine cluster and ^{19}F using SIMPSON [20] indicate that only a few locations of the ^{19}F relative to the plane defined by the three ^{13}C labels of the nearest-neighbor L-alanine are consistent with the observed relative RDX carbon dephasing ($\Delta S/S_0$, Fig. 4, bottom). Altogether calculations were performed for 412 ^{19}F positions and of these, only 39 had the correct order of relative dephasing for the three carbon peaks. Three views of the allowed positions are shown at the top of Fig. 4. All of these ^{19}F positions have the observed RDX dephasing ranking ($C_\alpha > CO > CH_3$), but not necessarily the correct relative dephasing rates. The better fits have the correct relative dephasing rates and are indicated by the darker spheres (smaller dimensionless RMSD values). These are not multi-parameter fits; rather, six experimental values of $\Delta S/S_0$ (from two spectra) were matched to calculated values by changing just a single parameter, the location of the ^{19}F label. The structure and all NMR parameters for the alanine cluster were fixed.

The RDX simulations included carbon–carbon homonuclear dipolar couplings calculated from the crystal structure of L-alanine [23], carbon CSA tensors [24], and isotropic J couplings [25,26]. In general, this sort of information about a cluster is readily available either from the literature, or from independent experiments on the cluster itself. The calculations were strongly dependent on the dipolar and isotropic J couplings, but only weakly dependent on the CSA tensors. The values for the alanine ^{13}C–^{13}C dipolar couplings used in the calculations were $D_{12} = 2121\,\text{Hz}$, $D_{13} = 475\,\text{Hz}$, and $D_{23} = 2164\,\text{Hz}$. The values for the scalar couplings were $^1J_{12} = 54\,\text{Hz}$, $^1J_{23} = 35\,\text{Hz}$, and $^2J_{13} = 2\,\text{Hz}$. The oscillations in the calculated $\Delta S/S_0$ as a function of time (Fig. 4) arose primarily from the homonuclear dipolar couplings. The oscillations were not dependent on the choice of the time-domain step size and essentially disappeared when all homonuclear dipolar couplings were set to zero.

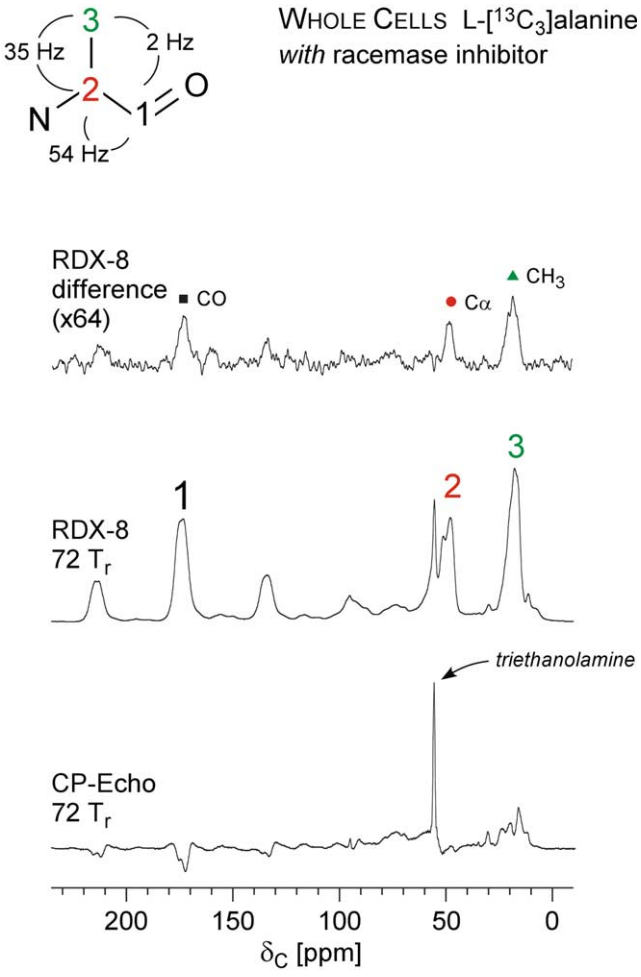

Fig. 3. $^{13}C\{^{19}F\}$ RDX spectra of mature whole cells of *S. aureus* labeled by L-[$^{13}C_3$]alanine and complexed to LY329332. The pulse sequence of Fig. 1 was used with magic-angle spinning at 5000 Hz and 72 rotor cycles of dipolar evolution. The RDX difference spectrum is shown at the top of the figure, and the full-echo spectrum just below. Data accumulation for the RDX spectra required 200,000 scans in nine days. The spectrum shown at the bottom of the figure was observed using a rotor-synchronized Hahn echo and the same evolution time. This spectrum is severely distorted by ^{13}C–^{13}C isotropic J couplings (inset) which were not refocused. The distortions complicate the proper phasing of overlapping natural-abundance ^{13}C peaks in the spectrum.

For convenience, the ^{19}F–^{13}CO distance was fixed at 7.6 Å. This value has been measured previously [21] in an isolated cell-wall complex with LY329332 using cells incorporating L-[1-^{13}C]alanine. Its use is not crucial. For example, recalculating the RDX dephasing with the

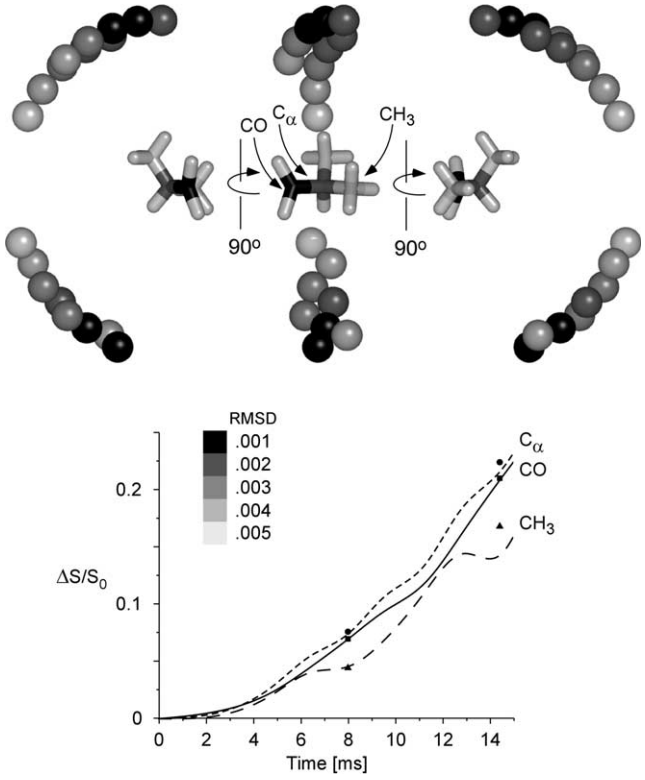

Fig. 4. $^{13}C\{^{19}F\}$ RDX experimental (symbols) and calculated (solid, dashed, and dotted lines, keyed to the alanine carbons) dephasing ($\Delta S/S_0$) for the whole-cell complex of Fig. 3. The RDX difference arises exclusively from alanine labels in the cell wall. The scale of the vertical axis is arbitrary. The dephasing for all three carbons at 14 ms relative to that at 8 ms has been scaled by a factor of 2.2. This factor arises from the observed shorter T_2 for cell-wall alanine labels than cytoplasmic alanine labels (see [20]). The scaling does not affect the relative dephasing rates. The calculated dephasing is for the ^{19}F positions represented by the gray-scale spheres shown in three views at the top of the figure. The more probable positions for the fluorine are indicated by darker shading.

black spheres in Fig. 4 but using a ^{13}CO–^{19}F distance of 5 Å, gave the observed relative dephasing rates (not shown). Thus, without a priori knowledge of the 7.6-Å alanine ^{13}CO–^{19}F distance, the *relative* distances of the three carbons of alanine to the ^{19}F can still be determined. We conclude that the RDX data fix the position of the ^{19}F relative to its nearest-neighbor L-alanine as closest to C_α and farthest from the CH_3.

3.1. Deuterium labeling and quadrupolar-echo REDOR

The determination of the orientation of dipolar and CSA tensors by REDOR is possible using the relative dephasing rates of chemical-shift sidebands [27]. In S{I} REDOR sideband dephasing experiments, for example, the orientation of the I-S vector relative to the S chemical-shift tensor is established [28]. If the alignment of the shift tensor in the molecular framework is known or can be inferred, then the I-S molecular geometry is defined. The same situation holds for the relative dephasing of quadrupolar spinning sidebands. Labeling with methyl-d_3 groups is particularly attractive because about six spinning sidebands are produced by convenient spinning speeds of 4–8 kHz.

If weak dipolar couplings between a dephasing nucleus and the observed ^2H labels are present, then long rotational-echo train lifetimes need to be maintained. This is the situation for the ^{19}F dephasing of whole-cell complexes of LY329332 and *S. aureus* grown on media containing L-[methyl-d_3]alanine in the presence of a racemase inhibitor. The nearest-neighbor ^{19}F–^2H distances are more than 8 Å, and therefore a total $\Delta S/S_0$ of substantially less than 10% will be observed even after 10 ms of REDOR dephasing [11,12]. This means that some sort of a pulsed echo-refocusing scheme must be used, even if the ^2H signal is on resonance, because the free induction decay following a ^2H inspection pulse disappears in about 5 ms (not shown). A ^2H π pulse in the middle of the evolution period will refocus chemical-shift offsets and provide full heteronuclear dipolar dephasing, but will not refocus dephasing due to a slightly mis-set magic angle, which may dominate the echo-train lifetime if large quadrupolar interactions are present.

A possibility in this situation is to use a quadrupolar echo (Fig. 5). A ^2H $\pi/2$ pulse in the middle of the evolution period will help refocus dephasing arising from an error in the setting of the magic angle, and will partially refocus chemical-shift offsets due to distributions of isotropic shifts. Even though the dephasing due to ^{19}F–^2H dipolar coupling is incomplete, clear differences in the relative dephasing rates of some of the spinning sidebands are observed (Fig. 6, left). Without further analysis, these differences in dephasing rates prove the existence of an orientational preference. A practical complication is that an unfortuitous choice of spinning speed can obscure the presence of local orientation (Fig. 6, right). Differences in the relative dephasing rates of the −1 and −2 sidebands are observed with spinning

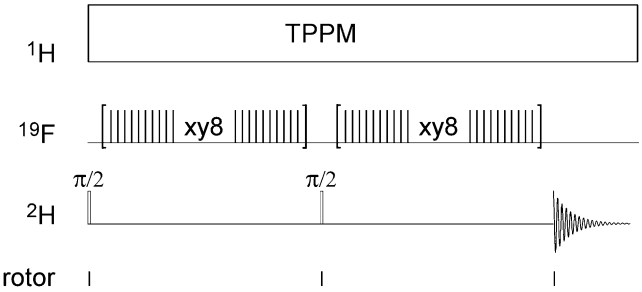

Fig. 5. $^2H\{^{19}F\}$ quadrupolar-echo REDOR sequence. A single ^2H $\pi/2$ pulse in the middle of the evolution period partially refocuses chemical-shift interactions and completely refocuses dephasing due to errors in setting the magic angle. All dephasing pulses are on the ^{19}F channel at the half and full rotor period. Phases of the ^{19}F pulses follow the standard xy8 alternation scheme. Two-pulse phase modulation of the ^1H RF is used throughout evolution and decoupling periods.

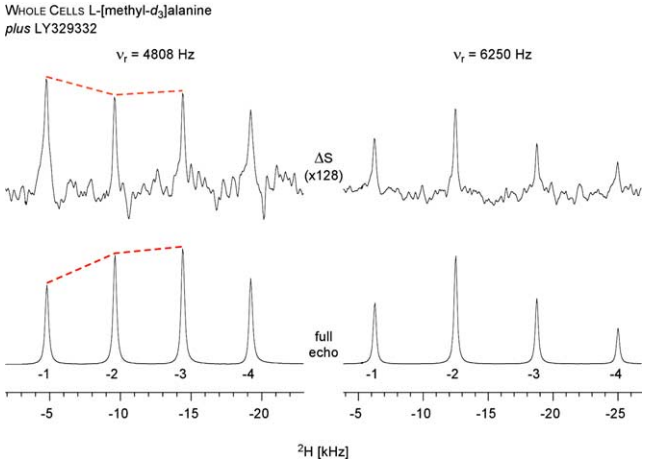

Fig. 6. $^2H\{^{19}F\}$ quadrupolar-echo REDOR spectra of mature whole cells of *S. aureus* labeled by L-[methyl-d_3]alanine and complexed to LY329332. The pulse sequence of Fig. 5 was used with magic-angle spinning at 4808 Hz (left) and 6250 Hz (right). Only the first four spinning sidebands are shown. The spectra have been symmetrized (and improved in sensitivity) by adding high-field and low-field spinning sidebands. The REDOR differences are shown at the top of the figure and the nominal full-echo spectra at the bottom. Data accumulation required 800,000 scans in three weeks for each set of REDOR spectra.

at 4804 Hz but not at 6250 Hz. This is an accident of the spatial averaging, which was confirmed by simulation.

Multi-spin simulations using SIMPSON [20] translate the observed orientational preference of Fig. 6 into the location of the ^{19}F on the surface of either of two cones centered on the methyl-d_3 (Fig. 7, cones). The ambiguity inherent in the presence of two cones rather than one is the result of the axial symmetry of the quadrupolar tensor. This ambiguity is removed by combining the $^2H\{^{19}F\}$ REDOR results with the $^{13}C_3\{^{19}F\}$ RDX results (Fig. 7, cones and spheres). Only two locations on one cone are consistent with the combination of results of both types of experiments. The structural details in Fig. 7 are now being used as restraints in molecular dynamics simulations aimed at generating a true molecular model of the binding site of LY329332 in the cell walls of mature cells of *S. aureus*. Experiments on dividing cells are in progress.

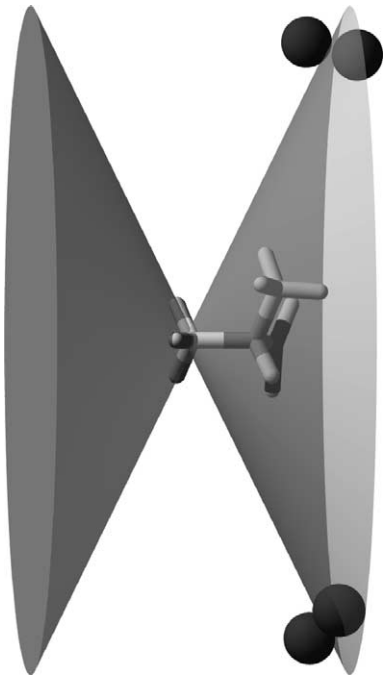

Fig. 7. Cones centered on the methyl-d_3 moiety of L-alanine on whose surfaces a ^{19}F would give rise to the $^2H\{^{19}F\}$ relative sideband dephasing of Fig. 6. Only the cone on the right intersects the arc of possible ^{19}F positions (spheres) described in Fig. 4 (top).

Acknowledgments

This work was supported by NIH Grant GM51554. The multi-spin simulations were done with software generously supplied by the laboratory of Professor Niels Chr. Nielsen (University of Aarhus). The authors thank Dr. Richard C. Thompson and Dr. Thalia I. Nicas (Lilly Research Laboratories, Indianapolis, IN) for providing samples of LY329332.

References

[1] T. Gullion, J. Schaefer, Adv. Magn. Reson. 13 (1989) 57.
[2] G. Tong, Y. Pan, H. Dong, R. Pryor, G.E. Wilson, J. Schaefer, Biochemistry 36 (1997) 9859.
[3] M.J. Rodriguez, N.J. Snyder, M.J. Zweifel, S.C. Wilkie, D.R. Stack, R.D. Cooper, T.I. Nicas, D.L. Muyllen, T.F. Butler, R.C. Thompson, J. Antibiot. (Tokyo) 51 (1998) 560.
[4] D.H. Williams, J. Kalman, J. Am. Chem. Soc. 99 (1977) 2768.
[5] J.C. Barna, D.H. Williams, Annu. Rev. Microbiol. 38 (1984) 339.
[6] P.E. Reynolds, Eur. J. Clin. Microbiol. Infect. Dis. 8 (1989) 943.
[7] J. Schaefer, R.A. McKay, US Patent 5,861,748 (1999).
[8] T. Gullion, D.B. Baker, M.S. Conradi, J. Magn. Reson. 89 (1990) 479.
[9] A.E. Bennett, C.M. Rienstra, M. Auger, K.V. Lakshmi, R.G. Griffin, J. Chem. Phys. 103 (1995) 6951.
[10] A.K. Mehta, J. Schaefer, J. Magn. Reson. 163 (2003).
[11] D.R. Studelska, C.A. Klug, D.D. Beusen, L.M. McDowell, J. Schaefer, J. Am. Chem. Soc. 118 (1996) 5476.
[12] L.M. McDowell, A. Schmidt, E.R. Cohen, D.A. Studelska, J. Schaefer, J. Mol. Biol. 256 (1996) 160.
[13] Y. Li, B. Poliks, L. Cegelski, M. Poliks, Z. Grycynski, G. Piszcek, P.G. Jagtap, D.R. Studelska, D.G.I. Kingston, J. Schaefer, S. Bane, Biochemistry 39 (2000) 281.
[14] J.J. Balbach, Y. Ishii, O.N. Antzutkin, R.D. Leapman, N.W. Rizzo, F. Dyda, J. Reed, R. Tycko, Biochemistry 39 (2000) 13748.
[15] J. Wang, Y.S. Balazs, L.K. Thompson, Biochemistry 36 (1997) 1699.
[16] S.O. Smith, T. Kawakami, M. Ziliox, S. Aimoto, J. Mol. Biol. 313 (2001) 1139.
[17] M.E. Merritt, A.M. Christensen, K.J. Kramer, T.L. Hopkins, J. Schaefer, J. Am. Chem. Soc. 118 (1996) 11278.
[18] Y. Pan, N.S. Shenouda, G.E. Wilson, J. Schaefer, J. Biol. Chem. 268 (1993) 18692.

[19] C.A. Michal, L.W. Jelinski, J. Biol. NMR 12 (1998) 231.
[20] M. Bak, J.T. Rasmussen, N.C. Nielsen, J. Magn. Reson. 147 (2000) 296.
[21] S.J. Kim, L. Cegelski, D.R. Studelska, R.D. O'Connor, A.K. Mehta, J. Schaefer, Biochemistry 41 (2002) 6967.
[22] C.P. Jaroniec, B.A. Tounge, J. Herzfeld, R.G. Griffin, J. Am. Chem. Soc. 123 (2001) 3507.
[23] M.S. Hehman, T.F. Koetzle, W.C. Hamilton, J. Am. Chem. Soc. 94 (1972) 2657.
[24] A. Naito, S. Ganapathy, K. Akasaka, C.A. McDowell, J. Chem. Phys. 74 (1981) 3190.
[25] S. Tran-Dinh, S. Fermandjian, E. Sula, R. Mernet-Bouvier, M. Cohen, P. Fromageot, J. Am. Chem. Soc. 96 (1974) 1484.
[26] R. Niedermeyer, R. Freeman, J. Magn. Reson. 30 (1978) 617.
[27] J.M. Goetz, J. Schaefer, J. Magn. Reson. 129 (1997) 222.
[28] R.D. O'Connor, J. Schaefer, J. Magn. Reson. 154 (2002) 46.